ORIGINAL RESEARCH

Paclitaxel-loaded nanobubble targeted to pro-gastrin-releasing peptide inhibits the growth of small cell lung cancer

Jin-Ping Wang[1,2]
Ji-Ping Yan[2]
Jing Xu[1]
Ting-Hui Yin[3]
Rong-Qin Zheng[3]
Wei Wang[1]

[1]Key Laboratory of Chemical Biology and Molecular Engineering of Ministry of Education, Institute of Biotechnology, Shanxi University, Taiyuan, Shanxi 030006, People's Republic of China; [2]Department of Ultrasound, Shanxi Province People's Hospital, Taiyuan, Shanxi 030012, People's Republic of China; [3]Department of Medical Ultrasonic, The Third Affiliated Hospital of Sun Yat-sen University, Guangzhou, Guangdong 510630, People's Republic of China

Correspondence: Ting-Hui Yin
Department of Medical Ultrasonic, The Third Affiliated Hospital of Sun Yat-sen University, Guangzhou, Guangdong 510630, People's Republic of China
Tel +86 208 525 2010
Fax +86 208 525 2010
Email yinth3@mail.sysu.edu.cn

Wei Wang
Key Laboratory of Chemical Biology and Molecular Engineering of Ministry of Education, Institute of Biotechnology, Shanxi University, 92 Wucheng Rd, Taiyuan, Shanxi 030006, People's Republic of China
Tel +86 351 496 0032
Fax +86 351 496 0032
Email gene@sxu.edu.cn

Objective: The aim of this work was to study the effects of paclitaxel-loaded nanobubbles targeting pro-gastrin-releasing peptide, designated as paclitaxel targeting nanobubbles, on small cell lung cancer (SCLC).

Methods: Paclitaxel targeting nanobubbles were prepared by Thin-film hydration method. Subsequently, the prepared nanomaterials were tested for their in vitro effects on SCLC H446 cells proliferation, apoptosis and motility using the CCK-8 assay, flow cytometry and cell scratch test. Next, the potential molecular regulatory mechanisms of the prepared nanomaterials on H446 cells were evaluated by RT-PCR, Western blot and immunohistochemical detection. Finally, the in vivo effects of the constructed nanomaterials were assessed on SCLC tumor using tumor-burdened nude mice models.

Results: Paclitaxel targeting nanobubbles significantly inhibited SCLC cell proliferation and migration, and promoted cell apoptosis. Moreover, the expression levels of Bcl-2, survivin, CDK2 and MMP-2 significantly decreased in SCLC cells treated with paclitaxel targeting nanobubbles, whereas the expression of caspase-3 and Rb were increased. There was a notable decrease in tumor size in vivo in SCLC nude mice models treated with paclitaxel targeting nanobubbles.

Conclusion: Paclitaxel targeting nanobubbles effectively inhibited the proliferation, migration and invasion of SCLC cells and induced SCLC cells apoptosis. Hence, these nanobubbles show potential in SCLC-targeted drug treatment application.

Keywords: paclitaxel, nanobubbles, proliferation, targeted therapy, small cell lung cancer

Introduction

Small cell lung cancer (SCLC) is a recalcitrant malignancy, which constitutes approximately 14% of all lung cancers.[1,2] Unlike non-small cell lung cancer (NSCLC), SCLC possesses the propensity for early metastases, and exquisite sensitivity to initial systemic cytotoxic chemotherapy.[3] Despite the high initial response to therapy, the 5-year survival rate is still below 7%. Notably, most SCLC patients eventually survive for only 1 year or less after diagnosis.[1,3,4] Systemic chemotherapy, as a bedrock treatment for SCLC, has reached a therapeutic efficacy plateau.[3] Advances in molecular profiling and development of targeted therapies witnessed with NSCLC in the last decade remain to be successfully replicated in SCLC. Hence, there is an urgent need for more effective SCLC treatment. In this vein, cancer-targeting drug therapy has become an exciting research field toward the treatment of SCLC.[2,3] Pro-gastrin-releasing peptide

(ProGRP), a stable precursor for gastrin-releasing peptide, is the most common, effective and specific biomarker for the diagnosis and treatment of SCLC.[5,6] For this reason, targeting ProGRP with the aim of inhibiting the growth of SCLC is a potential therapeutic intervention strategy.[7]

Paclitaxel, the prototype of the taxane class of chemotherapeutics, can suppress microtubule spindle dynamics and block metaphase–anaphase transitions, inhibit tumor cell mitosis, suppress cell proliferation and induce apoptosis.[8] Consequently, paclitaxel is widely used as a first-line treatment for various cancers, such as breast cancer, prostate cancer and NSCLC.[8,9] Due to poor aqueous solubility, paclitaxel is frequently solubilized in polyoxyethylated castor oil for clinical application. However, this formulation can easily cause systemic side effects and produce allergic reactions.[10] Thus, novel paclitaxel formulations have been developed, especially nano-drug delivery systems. Targeted nanoparticles drug delivery system has been widely applied to various cancer therapeutic approaches.[11,12] Indeed, some nano-drugs have entered clinical trials phases while similar advances in SCLC targeted nano-drug delivery system are few.

Therefore, we used the Thin-film hydration method to construct a new nano-drug delivery system, paclitaxel-loaded nanobubbles targeting ProGRP, designated as paclitaxel targeting nanobubbles. We then explored the effects and molecular mechanism of the constructed paclitaxel targeting nanobubbles on SCLC *in vitro* and in *vivo*.

Materials and methods
The preparation of paclitaxel targeting nanobubbles

Dipalmitoyl phosphatidylcholine (DPPC, 18 mg), diphenylphosphoryl azide (DPPA, 1 mg), 1,2-distearoylsn-glycero-3-phosphoethanolamine (DSPE, 1 mg) and paclitaxel (1 mg) were completely dissolved in 4 mL chloroform. Solvents were evaporated from the mixture in the fume hood to form a phospholipid film, followed by hydration in glycerol and PBS mixture (volume ratio, 1:9) in a shaking incubator at room temperature for 1 hr to form paclitaxel-loaded liposomes. The liposomal suspension was collected and transferred to a 50 mL centrifuge tube for further analysis. The liposome concentration was determined using a phosphorus assay. Ten microgram of anti-Pro GRP monoclonal antibody (anti-ProGRP monoclonal antibody) was prepared as previously described,[4] diluted with 50 μL of PBS, and added to 10 μL EDTA (0.5 M). This solution was then incubated with

mercaptoethylamine (50 mg), EDTA (10 μL, 0.5 M) and PBS (500 μL) at 37°C for 90 mins. To form single-chain anti-Pro GRP antibody (scAb), the mixture was centrifuged three times (3,000 rpm, 8 mins, 4°C) with 500 μL of PBS containing EDTA (10 μL, 0.5M). Thereafter, the scAb and liposomes (500 μL, 5 μg/mL) were incubated at 4°C overnight, centrifuged with PBS to remove the free antibody, and re-suspended in 0.5 mL of PBS. The samples were then slowly injected into the solution of ventilation with 10 mL perfluorinated propane gas (C_3F_8) using sterile syringe injection (Tianjin Physical and Chemical Engineering Institute of Nuclear Industry), shaken with capsule silver mercury device for 45 s (Tiancheng Technology Co., LTD.), and left to stand gently. The upper level bubble of this mixture was discarded to leave the residual milky suspension containing paclitaxel targeting nanobubbles (both paclitaxel and anti-ProGRP monoclonal antibody loaded liposomal nanobubbles). The procedures are shown in Figure 6. In addition, C_3F_8 injected paclitaxel liposome was only paclitaxel-loaded nanobubbles, named as nanobubbles carrying paclitaxel.

Paclitaxel quantitative determination
The concentration of paclitaxel was determined using HPLC fitted with a reverse phase Agilent TC C18 column (150mm ×4.6 mm, 5 μm, Agilent Technologies, CA, USA) and a UV detector capable of scanning a wavelength range of 200–600 nm. Mobile phase system comprising acetonitrile and water (60:40 v/v) at a flow rate of 1 mL/min was employed for elution. Paclitaxel was measured at a wavelength of 227 nm, and its concentration calculated using the external standard method. For this purpose, 1 mg of paclitaxel dissolved in a volumetric flask using acetonitrile to obtain a stock standard solution. The stock solution was then diluted using mobile phase to yield a series of calibration solutions analyzed by the HPLC system. A linear calibration curve was obtained over the concentration range of 0.5–25 μg/mL of paclitaxel with a regression coefficient of 0.998.

Encapsulation efficiency and loading capacity of paclitaxel in nanobubbles
Paclitaxel targeting nanobubbles or nanobubbles carrying paclitaxel were initially dissolved in 0.1 mL of acetonitrile before 0.8 mL of phosphate buffer (pH 6.0) was added to the solution. After shaking for 2 hrs, the resultant suspension was added to an Amicon® Ultra-0.5 centrifugal filter device and centrifuged at 10,000 rpm for 60 mins. The ultrafiltrate containing free paclitaxel was subsequently collected and

analyzed using the HPLC system to obtain the concentration of free paclitaxel. Consequently, the encapsulation efficiency was calculated using the following equation:

$$\text{Encapsulation efficiency} = [(\text{total amount of paclitaxel} - \text{amount of free paclitaxel})/\text{total amount of paclitaxel}] \times 100\%$$

Paclitaxel loading capacity was evaluated using freeze-dried nanobubbles. In brief, a predetermined amount of freeze-dried paclitaxel targeting nanobubbles was diluted in 5 mL of ethanol, followed by sonication and centrifugation. The supernatant that formed was removed and analyzed by HPLC. The loading capacity was then calculated using the following equation:

$$\text{Loading capacity} = [(\text{total amount of paclitaxel} - \text{amount of free paclitaxel})/\text{weight of nanobubbles}] \times 100\%$$

Paclitaxel release studies

In vitro, paclitaxel release studies were performed using a multi-compartment rotating cell comprising donor and receiver chambers, separated by a cellulose membrane permeable to substances below (cutoff =12,000 Da). One milliliter of paclitaxel targeting nanobubbles suspension was introduced into the donor chamber whereas phosphate buffer (1 mL, 0.05 M, pH 7.4) and 0.1% SDS, a mixture that could assure drug solubility, were added into the receiving chamber. At fixed time intervals, the contents in the receiving chamber were withdrawn, and replaced with fresh buffer mixture. The withdrawn samples were detected by HPLC to obtain the concentration of paclitaxel.

Characterization and stability of paclitaxel targeting nanobubbles

The morphology of paclitaxel targeting nanobubbles was determined by transmission electron microscopy (TEM, JEM-1011, Inc., Peabody, MA, USA). Samples for TEM analysis were prepared by depositing a drop of diluted paclitaxel targeting nanobubbles dispersion on the processed microvesicle copper net, dying with 3% negative phosphotungstic acid for 2 mins, and drying overnight. Additionally, the physical stability of paclitaxel targeting nanobubbles was measured for a period of 3 months by monitoring the average diameters of nanobubbles using a size and Zeta potential analyzer (90 plus/BI-MAS Brookhaven). Each diameter measurement was taken five times and the average calculated.

The effect of paclitaxel targeting nanobubbles on the proliferation of SCLC

The effect of paclitaxel targeting nanobubbles on SCLC cell proliferation was detected by CCK 8 assay. The H446 SCLC cells (Cat no. TCHu196) were purchased from the Cell Culture Bank of the Chinese Academy of Sciences (Shanghai, People's Republic of China) and cultured in RPMI-1640 medium containing 10% FBS. The culture mixture was maintained at 37°C and supplied with 5% CO_2. After cell growth reached logarithmic phase, cells were digested with pancreatic enzyme, beaten into a cell suspension liquid and re-suspended in medium containing 8% fetal bovine serum. Next, cells were seeded in 96-well culture plate at a density of 100–1,000 cells per well and then incubated overnight. Subsequently, H446 cells were separately exposed to four different materials (blank nanobubbles, paclitaxel, nanobubbles carrying paclitaxel or paclitaxel targeting nanobubbles) at 0.01, 0.1, 1, 10 and 50 µM concentrations and then incubated for 24 hrs. Next, 10 µL CCK 8 reagent was added to the cells and incubated for another 2–4 hrs. The resulting formazan precipitates were dissolved in DMSO and absorbance measured at 450 nm using a microplate reader (Thermo Scientific Microplate Reader, Thermo Fisher Scientific, Waltham, MA, USA).

The effects of paclitaxel targeting nanobubbles on the apoptosis of SCLC

The H446 SCLC cells were incubated separately with blank nanobubbles, paclitaxel, nanobubbles carrying paclitaxel or paclitaxel targeting nanobubbles at a paclitaxel drug concentration of 10 µM for 24 hrs. Thereafter, the cells were digested, centrifuged and suspended in 195 µL Annexin V-PE binding buffer. Afterward, Annexin V-PE (5 µL) was added to the cell suspensions and the mixture incubated in the dark at room temperature (20–25°C) for 10 mins. After this, the cells were digested, centrifuged and re-suspended in 200 µL of Annexin V-PE binding fluid and analyzed by flow cytometry (FACSCalibur, BD, Franklin Lake, NJ, USA).

The effect of paclitaxel targeting nanobubbles on the migration of SCLC

The cell scratch experiment was used to test the migration ability of tumor cells. All instruments were sterilized before operation. Cells were cultured in a 6-well plate at a density of 5×10^4 cells/well for 24 hrs. When cells grew into a single monolayer and reached more than 90% confluence, the sterilized plastic pipette tip (100 µL) was used

to draw a scratch in the monolayer cells. After washing away cell debris, the cells were incubated in complete medium separately containing blank nanobubbles, paclitaxel, nanobubbles carrying paclitaxel or paclitaxel targeting nanobubbles, for 36 hrs. Each media contained 10 μM of paclitaxel. Cell growth was monitored by taking photographs under a microscope at 0, 12, 24 and 36 hrs.

Quantitative real-time PCR (qRT-PCR) determination of the expression levels of Bcl-2, cyclin-dependent kinase (CDK2), survivin, matrix metalloproteinase-2 (MMP-2) and caspase-3 in SCLC cells

The H446 cells were treated separately with blank nanobubbles, paclitaxel, nanobubbles carrying paclitaxel or paclitaxel targeting nanobubbles for 24 hrs. Each of the materials contained 10 μM of paclitaxel. Total RNA was extracted using Trizol reagent according to the manufacturer's instructions. For the isolated RNA, cDNA was prepared using a Reverse Transcription Kit according to the manufacturer's protocol. Subsequent qRT-PCR analysis was carried out using the Fast SYBR green master mix on the Fast Real-Time PCR system (Applied Biosystems). The qRT-PCR reaction procedure was as shown: 95°C for 5 mins, 40 cycles of 92°C for 30 s, 60°C for 40 s, and 72°C for 1 min. Each experiment was repeated independently three times. Comparative quantification of these molecular levels was evaluated and normalized by the $2^{-\Delta\Delta Ct}$ method relative to β-actin. Primers sequences were as follows: BCL-2 forward: CGC ACC GGG CAT CTT CTC CTC, and reverse: GGA GAA GTC GTC GCC GGC CT; CDK2 forward: CCA GTA CTG CCA TCC GAG AG, and reverse: GTG AGA GCA GAG GCA TCC ATG; survivin forward: GGA CCA CCG CAT CTC TAC ATT C, and reverse: GTT CTC AGT GGG GCA GTG GAT G; MMP-2 forward: CCC AAG TGG GAC AAG AAC CAG ATC, and reverse: CAG CGG CCA AAG TTG ATC ATG; caspase-3 forward: GAT GTC GAT GCA GCA AAC CTC, and reverse: CAC CAT GGC TCA GAA GCA CAC.

Western blotting quantitation of the expression levels of Rb, caspase-3, survivin, CDK2 and Bcl-2 of SCLC cells

The H446 cells were treated separately with blank nanobubbles, paclitaxel, nanobubbles carrying paclitaxel and paclitaxel targeting nanobubbles for 24 hrs. In each case, 10 μM of paclitaxel was used. Subsequently, cells were

harvested and suspended in lysis buffer on ice for 30 mins, and centrifuged at 13,000×s g for 20 mins at 4°C. The supernatant was collected and the concentration of protein assessed by the bicinchoninic acid method. Equal amounts of proteins were loaded in SDS-PAGE and transferred to a PVDF membrane. Then, membranes were blocked in TBST containing 5% skimmed milk powder (Tris Buffered Saline Tween-20) for 1 hr, and incubated overnight with antibodies against Rb, caspase-3, survivin, CDK2, Bcl-2 and β-action. The membranes were then washed in TBST buffer and thereafter incubated with the corresponding horseradish peroxidase labeled second antibody for 1 hr at room temperature. After washing in TBST buffer, the membranes were visualized using the ECL detection system (Amersham Biosciences, Piscataway, NJ, USA). Protein bands were scanned using a light density scanner (Beckman Company, USA). Each experiment was performed in triplicates.

Construction of a tumor-burdened nude mice model

The BALB/c-nu male nude mice (4–5 weeks, 22.7±6.04 g) were obtained from Beijing Changyang Xishan Farm. This work was approved by Shanxi Medical University's Ethics Committee (Licence number: SYXK (Jin) 2015–0001). The experimental procedures were in compliance with the Care and Use of Laboratory Animals from the National Institutes of Health. The mice were raised in a temperature-controlled room (25–27°C, 40–50% humidity) on a 12 hrs light/dark cycle with free access to water and food. The H446 cells were cultured using RPMI-1640 medium with 10% FBS at 37°C with 5% CO_2 supply. The cells were collected during the logarithmic growth period and were re-suspended in PBS (pH=7.4) at a concentration of 1×10^7 cells/mL. A cell suspension (200 μL) was subcutaneously injected in the back of nude mice. Tumor development in the nude mice was monitored every 3 days and on day 10 after injection, the diameter of the tumors was about 1.0 cm, confirming that a tumor-burdened nude mice model had been successfully constructed.

Anti-tumor efficacy of paclitaxel targeting nanobubbles

The tumor-burdened nude mice were randomly divided into four groups each group comprising six mice. To each of the group of mice either blank nanobubbles, paclitaxel, nanobubbles carrying paclitaxel, or paclitaxel

targeting nanobubbles was administered at a dose of 1.32 mg/kg body weight by tail vein injection once a week for 4 consecutive weeks. The feeding and activity profiles of the mice were observed, and their weights recorded twice a week. Twenty-four days after initial administration of the respective drug materials, the tumors were removed from the mice, and their volume measured by a Vernier caliper. Additionally, the tumors were also prepared for further immunohistochemical analysis. Volume of tumors was calculated according to the formula:

$$\text{Tumor volume} = (a \times b^2)/2.$$

Parameters a and b refer to the length and width of the tumor, respectively.

Immunohistochemical analysis of the expression of Bcl-2, CDK2, survivin, caspase-3 and MMP-2 in SCLC tissues

The tumor tissues were successively treated using formaldehyde fixation, ethanol dehydration and paraffin embedding. The tissues were sliced and the sections dried overnight in the oven. Then, the paraffin wax was removed using xylene, ethanol, water and PBS, respectively. The tissue sections were then treated using 3% H_2O_2 in the dark for 10 mins and subsequently washed using distilled water and PBS three times consecutively. Antigens were retrieved using citrate buffer (pH 6.0) at 100°C for 10 mins and were washed with PBS three times. Each tissue section was incubated with primary antibodies against Bcl 2, CDK 2, survivin, caspase-3 and MMP-2 overnight at 4°C. Subsequently, each section was washed in PBS and incubated further using the secondary antibody at room temperature for 30 mins. After washing with PBS, each section was placed in 500 μL of diaminobenzidine solution at room temperature for 6 mins and washed in distilled water. Finally, each section was counterstained with hematoxylin, visualized and analyzed by use of a CX31 microscope (Olympus Corporation, Japan).

Statistical methods

The experimental data were obtained from at least three experiments and values expressed as mean±standard deviation. Statistical analysis was performed using the SPSS18.0 statistical software and differences between groups was evaluated using the Student's *t*-test. A value of *p* <0.05 was considered statistically significant.

Results
Physical properties of paclitaxel targeting nanobubbles

The physical properties of synthesized paclitaxel targeting nanobubbles were determined by HPLC, TEM and Zeta potential. Based on the HPLC results, the encapsulation efficiency and loading capacity of paclitaxel targeting nanobubbles were 70.72±5.38% and 3.29±0.17%, respectively. In comparison, the encapsulation efficiency and loading capacity of nanobubbles carrying paclitaxel were 68.98±4.56% and 2.91±0.13%, results which showed that paclitaxel could encapsulate equally well in targeted and non-targeted nanobubbles.

Regarding physical appearance, the paclitaxel targeting nanobubbles were a creamy white suspension and corresponding TEM images revealed their spherical shape and uniform distribution (Figure 1A and B). Moreover, the particle sizes (300–500 nm) in TEM were consistent with the values detected by a particle size analyzer (452.1±46.6 nm). The particle size distribution of paclitaxel targeting nanobubbles is listed in figure 1C. Additionally, these particles had a polydispersity index of 0.164±0.043 (Figure 1C) and Zeta potential of −15.8±2.72 mV (Figure 1D). In comparison, the parameters for nanobubbles carrying paclitaxel were: size (392±48.5 nm); polydispersity index (0.188±0.061) and Zeta potential (−17.3 ±3.35 mV).

The release profiles of paclitaxel targeting nanobubbles and nanobubbles carrying paclitaxel were detected *in vitro*. The results revealed prolonged *in vitro* release kinetics of paclitaxel from the two types of nanobubbles with no initial burst effect in both formulations. About 80% of the entrapped paclitaxel was released from paclitaxel targeting nanobubbles within the first 6 hrs, while 70% of the drug was released from nanobubbles carrying paclitaxel within the same period of time (Figure 1E, *p*<0.01).

The effect of paclitaxel targeting nanobubbles on the proliferation of SCLC cells

Biological effects of paclitaxel targeting nanobubbles were evaluated in SCLC cells using the CCK 8 assay. The H446 SCLC cells were first treated with four different materials
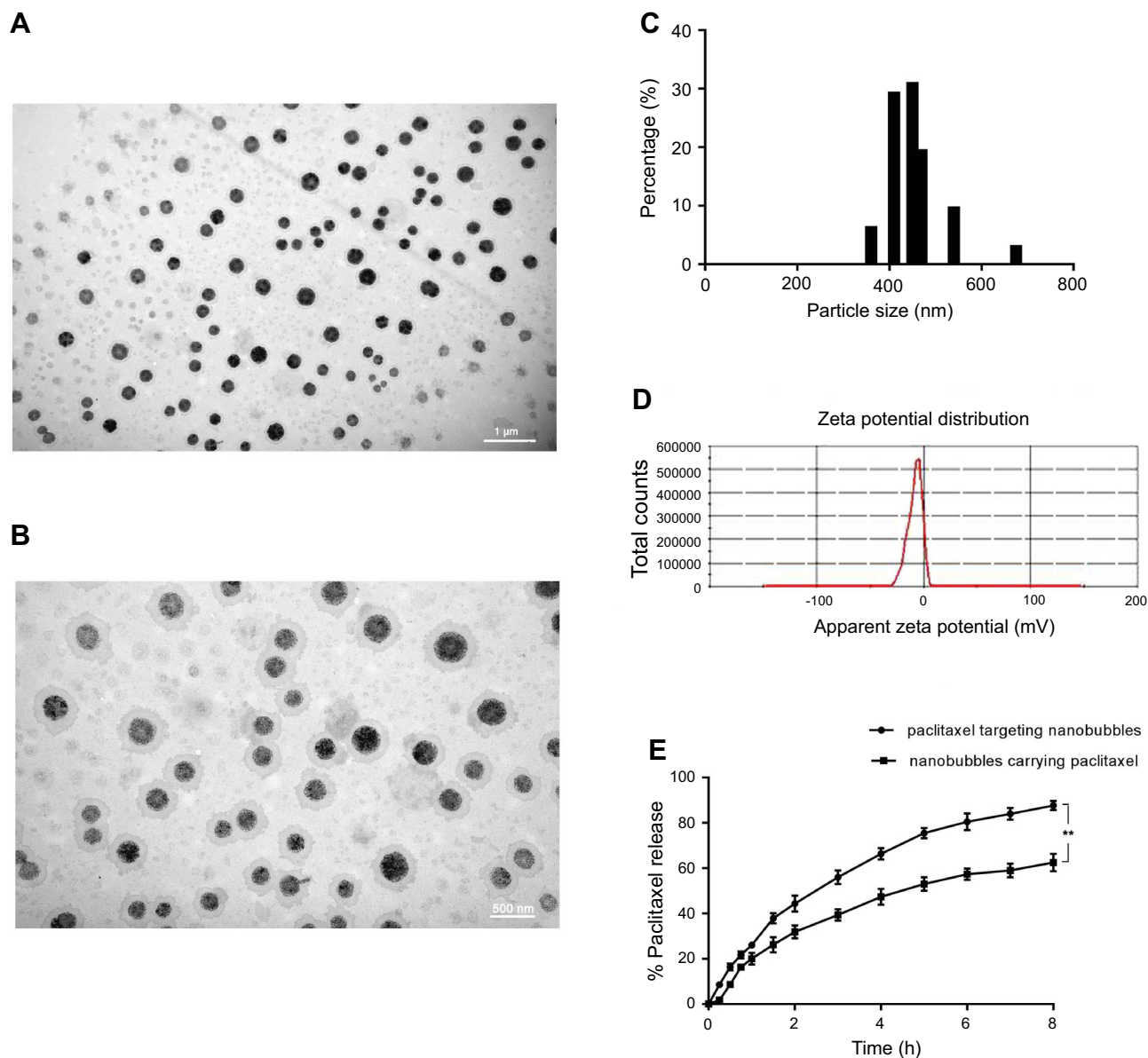
Figure 1 Electron microscopy image of paclitaxel targeting nanobubbles as detected by transmission electron microscopy. (**A**) Original magnification×3,000; (**B**) original magnification×6,000). (**C**) Particle size distribution of paclitaxel targeting nanobubbles as determined by laser particle size analysis. (**D**) Zeta potential of paclitaxel targeting nanobubbles. (**E**) *In vitro* paclitaxel release from paclitaxel targeting nanobubbles and nanobubbles carrying paclitaxel. **p<0.01.

(blank nanobubbles, paclitaxel, nanobubbles carrying paclitaxel or paclitaxel targeting nanobubbles), respectively. Each material was confected into different concentration solution (0.01, 0.1, 1, 10 and 50 μM). After administration for 24 hrs, the proliferation of H446 cells was determined by CCK 8. Paclitaxel, nanobubbles carrying paclitaxel and paclitaxel targeting nanobubbles could inhibit the viability of H446 cells in a dose-dependent manner (Figure 2A). Moreover, the greatest inhibitory effects were displayed by the paclitaxel targeting nanobubbles group. Besides, 10 μM of the drug, a highly effective

and low toxicity dose, was used in the following experiments. The results indicated that paclitaxel targeting nanobubbles could significantly inhibit the proliferation of H446 cells.

Effects of paclitaxel targeting nanobubbles on SCLC cells apoptosis

Apoptosis-inducing effects of paclitaxel targeting nanobubbles on H446 cells apoptosis were assessed quantitatively by flow cytometry. Compared to the other groups (Figure 2B and C): blank nanobubbles (2.68±1.1%);
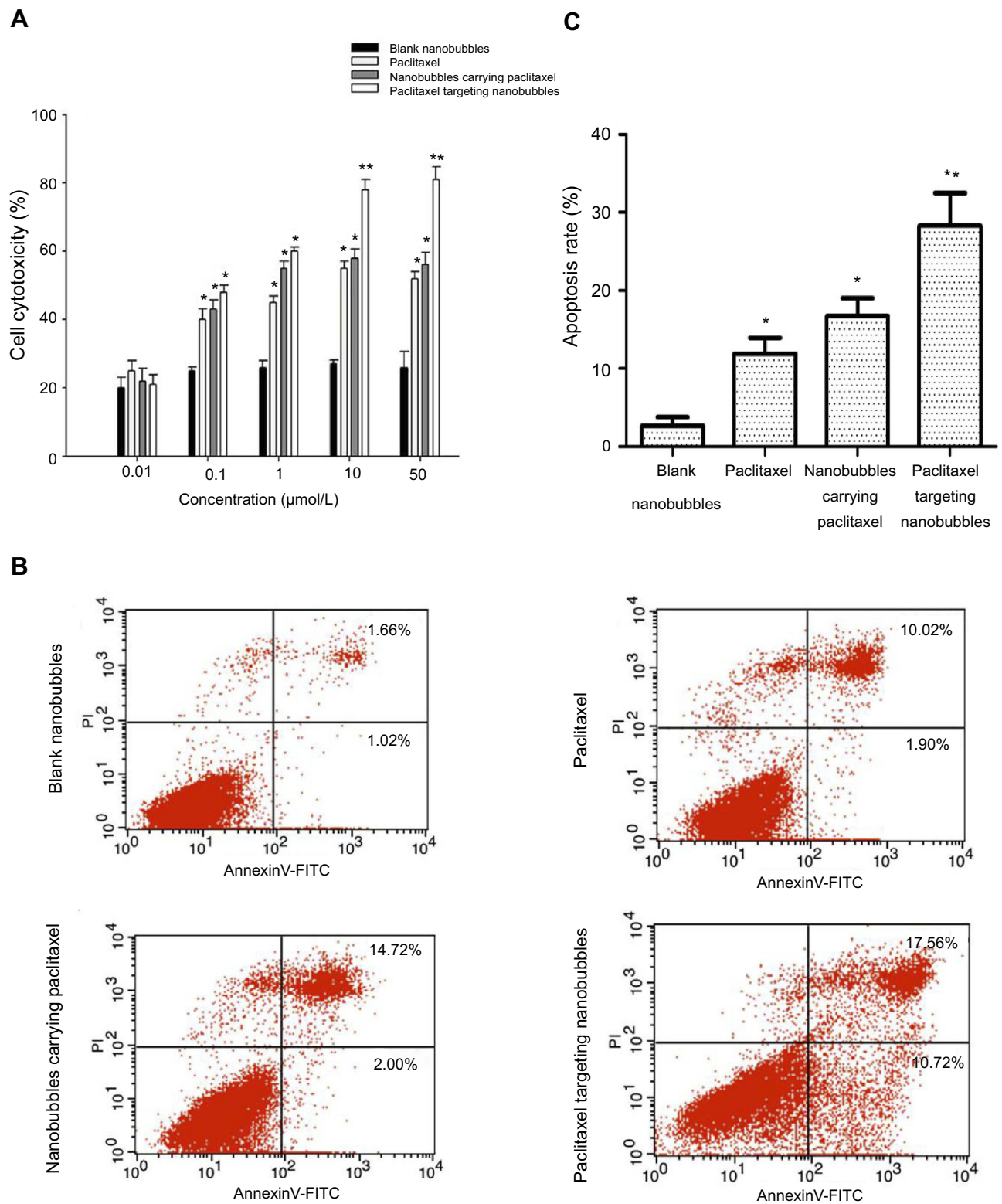
A

C

B

Figure 2 (**A**) Dose-dependent effect of paclitaxel targeting nanobubbles on the proliferation of H446 cells as measured using the CCK-8 assay. The drug in each group had different concentrations (0.01, 0.1, 1, 10 and 50 μM). 10 μM of the drug in each group was applied for further experiments. (**B**) The effect of paclitaxel targeting nanobubbles on apoptosis of H446 cells was determined by flow cytometry. (**C**) Quantitative analysis of apoptosis rate for different nanobubbles and paclitaxel. *$p<0.05$, **$p<0.01$.
Abbreviation: FITC, fluorescein isothiocyante.

paclitaxel (11.92±2.0%) and nanobubbles carrying paclitaxel (16.72±2.3%), marked apoptosis was observed with paclitaxel targeting nanobubbles (28.28±4.2%, $p<0.05$). Hence, paclitaxel targeting nanobubbles markedly induced the apoptosis of H446 cells ($p<0.05$, Figure 2B and C).

Evaluation of effects on the migration of SCLC cells

To explore the effects of paclitaxel targeting nanobubbles on the motility of H446 cells, we used the cell scratch experiment to measure cell migration. Accordingly, the H446 cells were treated with blank nanobubbles, paclitaxel, nanobubbles carrying paclitaxel or paclitaxel targeting nanobubbles and images of cell migration recorded every 12 hrs. A time-dependent decrease in the scratching distance was observed in the four groups (Figure 3). Moreover, the paclitaxel targeting nanobubbles displayed the greatest inhibition of H446 cells migration. Therefore, paclitaxel targeting nanobubbles could effectively inhibit the migration of H446 cells.

Evaluating molecular mechanisms mediating effects of paclitaxel targeting nanobubbles on SCLC

To investigate the potential molecular mechanisms at play in the observed effects of paclitaxel targeting nanobubbles on SCLC, qRT-PCR and Western blot were used to determine the expression of Bcl-2, CDK2, survivin, MMP-2, and caspase-3 in H446 cells. Besides, immunohistochemistry was applied to measure the expression of these molecules in vivo. In qRT-PCR, as compared to the blank nanobubbles control group, the expression levels of BCL-2, CDK2 and survivin were downregulated in paclitaxel group, nanobubbles carrying paclitaxel group and paclitaxel targeting nanobubbles group. In contrast, the expression of caspase-3 was upregulated in these groups. In each case, the changes produced by the paclitaxel targeting nanobubbles were significantly different from the others ($p<0.01$) (Figure 4A). On the other hand, MMP-2 gene expression showed no significant difference between the treatment groups and the control group containing blank nanobubbles.

In Western blot, the expression levels of BCL-2, CDK2 and survivin proteins were considerably downregulated in paclitaxel targeting nanobubbles group compared with the blank nanobubbles group, whereas the expression levels of Rb and caspase-3 proteins were evidently upregulated

(Figure 4B). The Western blot results were consistent with those obtained using qRT-PCR.

To further investigate the potential mechanism of paclitaxel targeting nanobubbles on SCLC, the expression levels of molecules in SCLC tumors obtained from the tumor-burdened nude mice models were determined by immunohistochemistry. The expression levels of BCL-2, CDK2, survivin and MMP-2 proteins showed an obvious decrease in paclitaxel targeting nanobubbles group when compared with the blank nanobubbles group, while the expression levels of caspase-3 proteins showed an obvious increase ($p<0.05$) (Figure 4C and D).

BCL-2, caspase-3, survivin, Rb, CDK2 and MMP-2 have different roles on cell apoptosis, cycle progression, proliferation and metastasis. Therefore, the results showed that paclitaxel targeting nanobubbles significantly inhibited the proliferation and migration of H446 cells and induced the apoptosis of H446 cells through regulating those biomolecules expression.

The anti-tumor efficacy of paclitaxel targeting nanobubbles on SCLC mice

In vivo effects of paclitaxel targeting nanobubbles on SCLC were assessed in tumor-burdened nude mice models. The nude mice were randomly divided into four groups as defined previously with six mice in each group. Changes in the volumes of tumors were monitored every 3days. The animal tumor volumes in the paclitaxel targeting nanobubbles group were significantly lower than that in the control group (Figure 5A–C). After removing the tumor, the results indicated that nude mouse tumor weight of paclitaxel targeting nanobubbles group was significantly lower than the control group ($p=0.001$, Figure 5D). Hence, paclitaxel targeting nanobubbles could markedly inhibit the growth of SCLC in vivo.

Discussion

This work indicated that paclitaxel targeting nanobubbles could effectively inhibit the proliferation and migration of SCLC cells, induce the apoptosis of SCLC cells and suppress the growth of tumors in tumor-burdened nude mice, which might be through regulating the expression of BCL-2, caspase-3, survivin, Rb, CDK2 and MMP-2. Hence, paclitaxel targeting nanobubbles had a good anti-tumor effect on SCLC.

There is convincing evidence suggesting that patients with SCLC treated using systemic chemotherapy still have
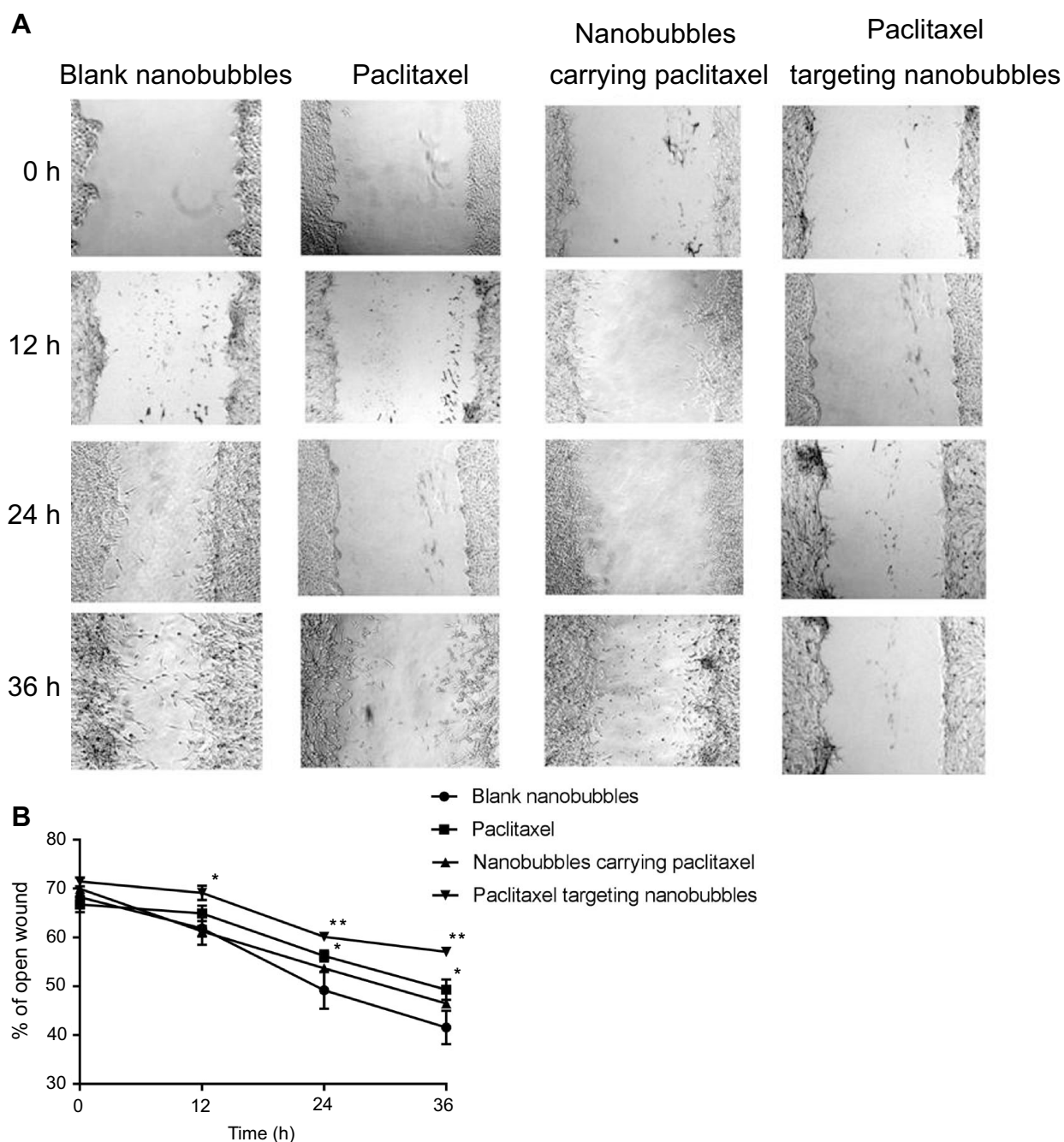
A

B

Figure 3 Effect of paclitaxel targeting nanobubbles on migration of H446 cells as determined using the cell scratch experiment. The images (**A**) and quantification analysis (**B**) of cell monolayer wound width are listed. 10 μM of the drug in each group was used. *$p<0.05$, **$p<0.01$.

low survival rates.[1,3] Thus, highly efficient and safe therapeutic methods for SCLC are urgently needed. Targeted therapy, in particular, the approach involving ProGRP, has attracted considerable attention in the treatment of SCLC because ProGRP is considered as the most effective diagnostic and therapeutic biomarker for SCLC.[7,13,14] Paclitaxel exerts very good anti-tumor effects on various cancers[8,9] but its clinical application is limited due to poor aqueous solubility.[10] Liposomes can encapsulate hydrophobic drugs

and enhance the bioavailability of drugs at the targeted site of action and also lower their toxicity.[15] In this study, we constructed a new nano-drug delivery system comprising both paclitaxel and anti-ProGRP monoclonal antibody loaded liposomal nanobubbles and investigated their potential use in the treatment of SCLC. These ProGRP-targeting nanobubbles, designated as paclitaxel targeting nanobubbles, displayed good aqueous solubility, high drug-loading rates and stability. Compared with blank nanobubbles, paclitaxel and
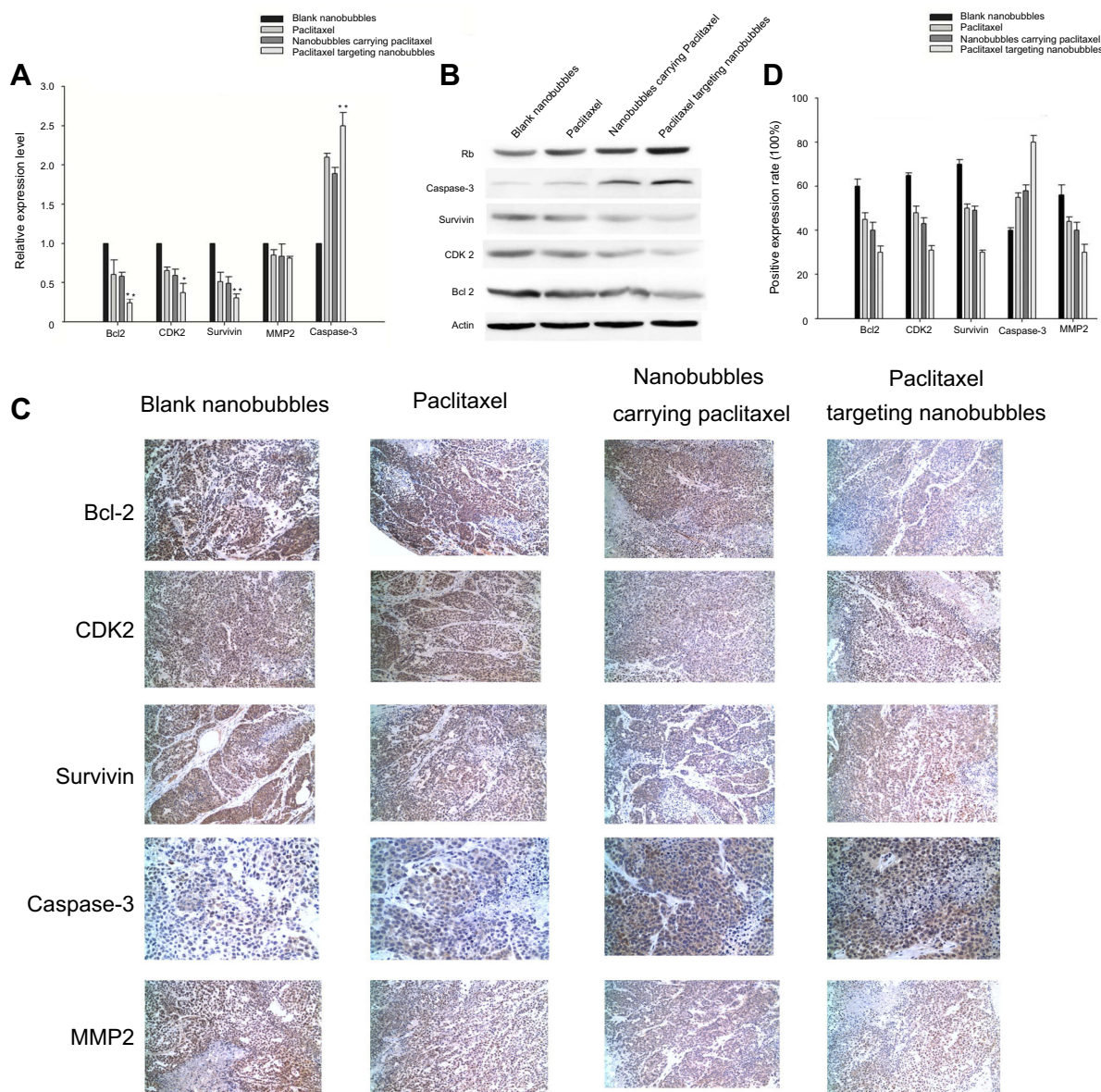
Figure 4 Determination of the molecular mechanism of paclitaxel targeting nanobubbles on SCLC. (**A**) qRT-PCR was used to evaluate the expression of Bcl-2, CDK2, survivin, MMP2 and caspase-3 in SCLC cells using 10 μM of drug in each group. (**B**) Western blot was applied to measure the expression of Rb, caspase-3, survivin, CDK2 and Bcl-2 in SCLC cells using 10 μM of drug in each group. (**C, D**) Immunohistochemical analysis was used to measure the expression of Bcl-2, CDK2, survivin, caspase-3, and MMP-2 in SCLC tumors. Drug was administered by tail vein injection at a dose of 1.32 mg/(kg body weight). *$p<0.05$, **$p<0.01$.

nanobubbles carrying paclitaxel, paclitaxel targeting nanobubbles significantly inhibited the proliferation and migration of SCLC H446 cells, induced the apoptosis of H446 cells, and suppressed the growth of SCLC tumors. In view of the results obtained in the study, targeting ProGRP could enhance the inhibition of paclitaxel-loaded nanobubbles on SCLC, making paclitaxel targeting nanobubbles as a potential therapeutic approach for SCLC.

The emergence of targeted therapy has been a significant breakthrough in cancer treatment, because targeted therapy can interfere with specific molecules in

tumor area to inhibit the progression of various cancers, thereby reducing injury to normal tissues.[16] For example, folate-targeting methods were applied to enhance the therapeutic effect of photo-thermo-radiotherapy in mouth epidermal carcinoma.[17] In the current study, targeting ProGRP could significantly promote the inhibition effects of paclitaxel-loaded nanobubbles on SCLC. Additionally, the improved aqueous solubility of paclitaxel targeting nanobubbles suggests that using liposomal nanobubbles as hydrophobic drug vehicles is a good option, although there are many publications reporting other polymeric

A Blank nanobubbles   Paclitaxel   Nanobubbles carrying paclitaxel   Paclitaxel targeting nanobubbles
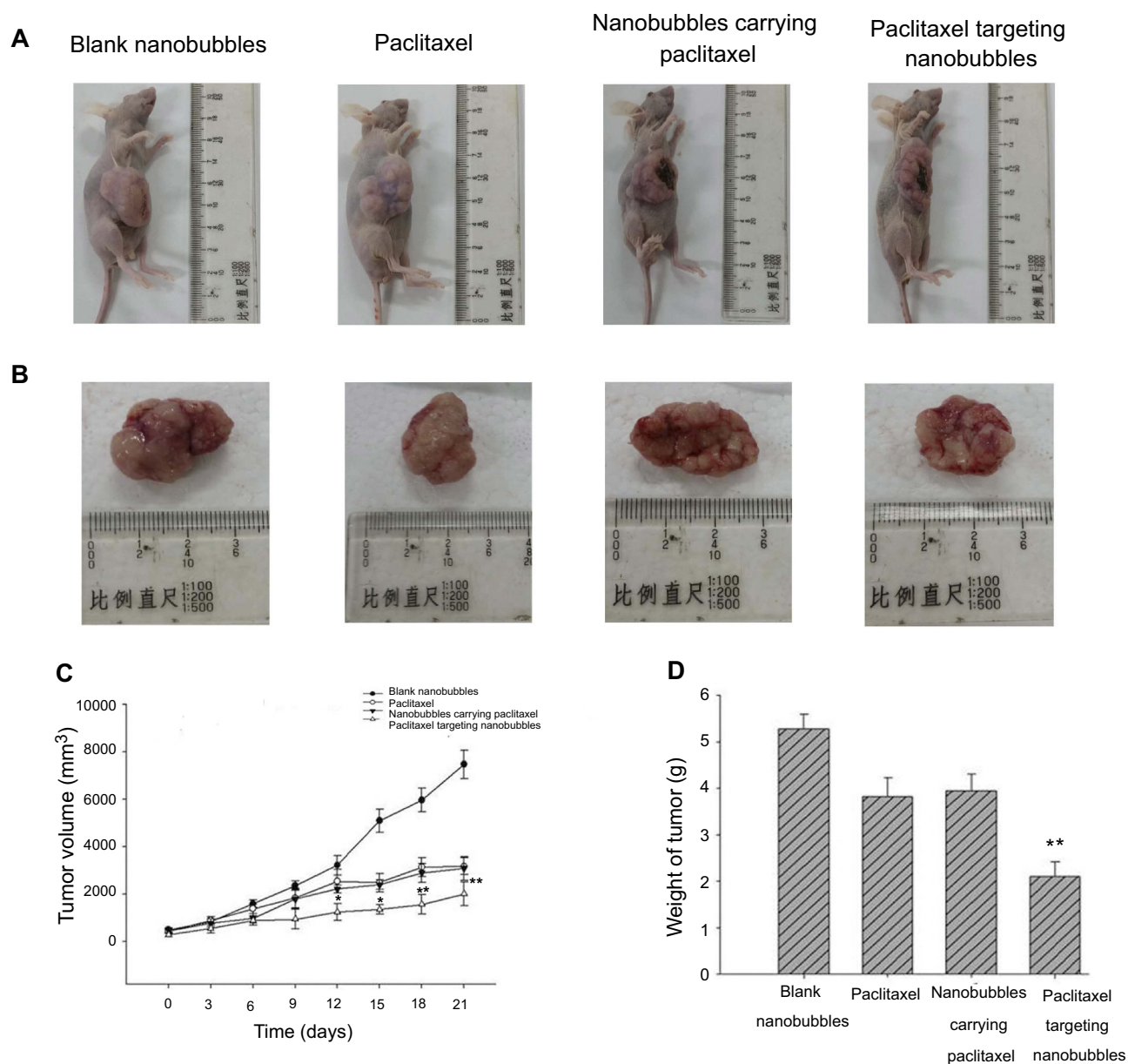

B

Figure 5 Assessment of the anti-tumor efficacy of paclitaxel targeting nanobubbles on SCLC mice. The role of nano-materials was observed through the change in tumor diameter (**A**, **B**); change in tumor volume (**C**), and change in tumor weight (**D**). *$p<0.05$, **$p<0.01$.

nanostructures as the effective drug carriers.[18] For instance, peptide 2 was able to inhibit SCLC growth but its potential was limited due to low aqueous solubility.[19] The solubility challenge could be circumvented by embedding the drug in a lipid bilayer and applying the targeted approach as explored in this study using paclitaxel targeting nanobubbles. Biomolecules play important roles in regulating various events of cell biological processes. For example, CDK2 is a serine/threonine protein kinase that regulates G1/S phase transition and S phase progression, which is essential for the control of cell cycle and proliferation.[20,21] The overexpression of CDK2 could lead to the abnormal

regulation of the cell cycle, which is markedly related to the hyper-proliferation of cancer cells, such as human lung cancer cell.[20,22,23] Research studies show that downregulation in the expression of CDK2 could considerably inhibit the proliferation of lung cancer cells.[23,24] In the present study, CDK2 expression in SCLC cells was downregulated after the administration of paclitaxel targeting nanobubbles. Retinoblastoma (Rb) gene is another biomolecule also known as a tumor suppressor gene which, together with the protein that it encodes for, has been identified as a common cell cycle regulator.[25,26] A loss of Rb function can allow unregulated cell cycle progression and promote
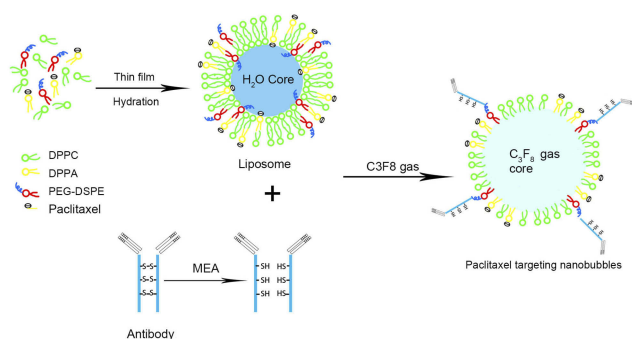
Figure 6 Schematic illustration for the synthesis of paclitaxel targeting nanobubbles.
Abbreviations: DPPC: dipalmitoyl phosphatidylcholine; DPPA: diphenylphosphor-ylazide; DSPE: 1,2-distearoylsn-glycero-3-phosphoethanolamine; PEG: polyethylene glycol; C3F8: perfluorinated propane gas; MEA: mercaptoethylamine

tumor growth, which is a frequent event in cancer including SCLC.[26–29] In this study, an upregulation in Rb expression was evident in the administration of paclitaxel targeting nanobubbles. MMP-2 is a zinc-dependent proteinase that degrades components of extracellular matrixsubstrates.[30] Thus, MMP-2 is critical for cell migration and invasion during physiological and pathological processes.[30,31] Overexpression of MMP-2 has been reported in lung cancer,[32] a finding consistent with observations from our study. Following treatment using paclitaxel targeting nano-bubbles, the expression levels of MMP-2 decreased. Therefore, paclitaxel targeting nanobubbles could inhibit the proliferation of SCLC H446 cells by regulating the expression of CDK2 and Rb, and suppress the migration of SCLC H446 cells via decreasing MMP-2 expression.

Apoptosis is a complex programmed cell death, which is regulated by a series of molecules such as survivin, Bcl-2 and caspase-3.[33,34] Defects in apoptosis can allow cells to survive and thus cause cancer or autoimmune disorders.[34] Survivin, an inhibitor of apoptosis protein, is highly expressed in most human malignancies, and its expression levels correlate with a poor clinical outcome.[35,36] It is reported that survivin is overexpressed in almost all human cancers, such as lung cancer, breast cancer and bladder cancer.[36] Bcl-2, an anti-apoptosis protein, is trans-located and overexpressed in tumors.[37,38] On the other hand, caspase-3, a pro-apoptosis protein, is a typical hall-mark of apoptosis and plays an important role in cell apoptotic chromatin condensation and DNA fragmentation.[39,40] Our study showed that paclitaxel target-ing nanobubbles administered to SCLC H446 cells could decrease the expression of survivin and Bcl-2 and enhance caspase-3 expression, thereby promoting cell apoptosis.

In conclusion, paclitaxel targeting nanobubbles could inhibit the growth of SCLC by regulating the expression of several biomolecules. Thus, paclitaxel targeting nanobub-bles may be a potential anti-cancer treatment strategy for SCLC. Further preclinical studies, including the use of diverse cell lines and clinical trials, will be required to validate these findings.

Acknowledgments

Disclosure

The authors report no conflicts of interest in this work.

References

1. Byers LA, Rudin CM. Small cell lung cancer: where do we go from here? *Cancer*. 2015;121:664–672. doi:10.1002/cncr.29098
2. Guohua H, Hongyang L, Zhiming J, Danhua Z, Haifang W. Study of small-cell lung cancer cell-based sensor and its applications in che-motherapy effects rapid evaluation for anticancer drugs. *Biosens Bioelectron*. 2017;97:184–195. doi:10.1016/j.bios.2017.05.050
3. Pillai RN, Owonikoko TK. Small cell lung cancer: therapies and targets. *Semin Oncol*. 2014;41:133–142. doi:10.1053/j.seminoncol.2013.12.015
4. Wang JP, Zhou XL, Yan JP, Zheng RQ, Wang W. Nanobubbles as ultrasound contrast agent for facilitating small cell lung cancer imaging. *Oncotarget*. 2017;8:78153–78162. doi:10.18632/oncotarget.18155
5. Huang Z, Xu D, Zhang F, Ying Y, Song L. Pro-gastrin-releasing peptide and neuron-specific enolase: useful predictors of response to chemotherapy and survival in patients with small cell lung cancer. *Clin Transl Oncol*. 2016;18:1019–1025. doi:10.1007/s12094-015-1479-4
6. Kiseli M, Caglar GS, Gursoy AY, et al. Pro-gastrin releasing peptide: a new serum marker for endometrioid adenocarcinoma. *Gynecol Obstet Invest*. 2018;83:540–545. doi:10.1159/000488854
7. Gong Z, Lu R, Xie S, et al. Overexpression of pro-gastrin releasing peptide promotes the cell proliferation and progression in small cell lung cancer. *Biochem Biophys Res Commun*. 2016;479:312–318. doi:10.1016/j.bbrc.2016.09.066
8. Khanna C, Rosenberg M, Vail DM. A review of paclitaxel and novel formulations including those suitable for use in dogs. *J Vet Intern Med*. 2015;29:1006–1012. doi:10.1111/jvim.12596
9. Hirsh V. nab-paclitaxel for the management of patients with advanced non-small-cell lung cancer. *Expert Rev Anticancer Ther*. 2014;14:129–141. doi:10.1586/14737140.2014.881719
10. Ma WW, Hidalgo M. The winning formulation: the development of paclitaxel in pancreatic cancer. *Clin Cancer Res*. 2013;19:5572–5579. doi:10.1158/1078-0432.CCR-13-1356
11. Kumari P, Ghosh B, Biswas S. Nanocarriers for cancer-targeted drug delivery. *J Drug Target*. 2016;24:179–191. doi:10.3109/1061186X.2015.1051049
12. Jain V, Jain S, Mahajan SC. Nanomedicines based drug delivery systems for anti-cancer targeting and treatment. *Curr Drug Deliv*. 2015;12:177–191.

13. Liu Z, Zhou X, Shi Y, et al. Study on biodistribution and radio-immunoimaging of (131)iodine-labeled monoclonal antibody D-D3 against progastrin-releasing peptide31–98 in tumor-bearing mouse. *Cancer Biother Radiopharm*. 2011;26:229–235. doi:10.1089/cbr.2010.0855

14. Holdenrieder S, von Pawel J, Dankelmann E, et al. Nucleosomes, ProGRP, NSE, CYFRA 21-1, and CEA in monitoring first-line chemotherapy of small cell lung cancer. *Clin Cancer Res*. 2008;14:7813–7821. doi:10.1158/1078-0432.CCR-08-0678

15. Shen Y, Pi Z, Yan F, et al. Enhanced delivery of paclitaxel liposomes using focused ultrasound with microbubbles for treating nude mice bearing intracranial glioblastoma xenografts. *Int J Nanomedicine*. 2017;12:5613–5629. doi:10.2147/IJN.S136401

16. Baudino TA. Targeted cancer therapy: the next generation of cancer treatment. *Curr Drug Discov Technol*. 2015;12:3–20.

17. Neshastehriz A, Tabei M, Maleki S, Eynali S, Shakeri-Zadeh A. Photothermal therapy using folate conjugated gold nanoparticles enhances the effects of 6MV X-ray on mouth epidermal carcinoma cells. *J Photochem Photobiol B*. 2017;172:52–60. doi:10.1016/j.jphotobiol.2017.05.012

18. Keshavarz M, Moloudi K, Paydar R, et al. Alginate hydrogel co-loaded with cisplatin and gold nanoparticles for computed tomography image-guided chemotherapy. *J Biomater Appl*. 2018;33:161–169. doi:10.1177/0885328218782355

19. Offerman SC, Kadirvel M, Abusara OH, et al. N-tert-Prenylation of the indole ring improves the cytotoxicity of a short antagonist G analogue against small cell lung cancer. *Medchemcomm*. 2017;8:551–558. doi:10.1039/c6md00691d

20. Shi XN, Li H, Yao H, et al. Adapalene inhibits the activity of cyclin-dependent kinase 2 in colorectal carcinoma. *Mol Med Rep*. 2015;12:6501–6508. doi:10.3892/mmr.2015.4310

21. Jin YH, Yim H, Park JH, Lee SK. Cdk2 activity is associated with depolarization of mitochondrial membrane potential during apoptosis. *Biochem Biophys Res Commun*. 2003;305:974–980.

22. Chohan TA, Qian H, Pan Y, Chen JZ. Cyclin-dependent kinase-2 as a target for cancer therapy: progress in the development of CDK2 inhibitors as anti-cancer agents. *Curr Med Chem*. 2015;22:237–263.

23. Xu L, Wang C, Wen Z, et al. Selective up-regulation of CDK2 is critical for TLR9 signaling stimulated proliferation of human lung cancer cell. *Immunol Lett*. 2010;127:93–99. doi:10.1016/j.imlet.2009.10.002

24. Sun M, Jiang R, Wang G, et al. Cyclin-dependent kinase 2-associated protein 1 suppresses growth and tumorigenesis of lung cancer. *Int J Oncol*. 2013;42:1376–1382. doi:10.3892/ijo.2013.1813

25. Rubin SM, Sage J. Defining a new vision for the retinoblastoma gene: report from the 3rd international Rb meeting. *Cell Div*. 2013;8:13. doi:10.1186/1747-1028-8-6

26. Hutcheson J, Witkiewicz AK, Knudsen ES. The RB tumor suppressor at the intersection of proliferation and immunity: relevance to disease immune evasion and immunotherapy. *Cell Cycle*. 2015;14:3812–3819. doi:10.1080/15384101.2015.1010922

27. Dick FA, Rubin SM. Molecular mechanisms underlying RB protein function. *Nat Rev Mol Cell Biol*. 2013;14:297–306. doi:10.1038/nrm3567

28. Meder L, Konig K, Ozretic L, et al. NOTCH, ASCL1, p53 and RB alterations define an alternative pathway driving neuroendocrine and small cell lung carcinomas. *Int J Cancer*. 2016;138:927–938. doi:10.1002/ijc.29835

29. Niederst MJ, Sequist LV, Poirier JT, et al. RB loss in resistant EGFR mutant lung adenocarcinomas that transform to small-cell lung cancer. *Nat Commun*. 2015;6:6377. doi:10.1038/ncomms7377

30. Jezierska A, Motyl T. Matrix metalloproteinase-2 involvement in breast cancer progression: a mini-review. *Med Sci Monit*. 2009;15:Ra32–Ra40.

31. Chien MH, Lin CW, Cheng CW, Wen YC, Yang SF. Matrix metalloproteinase-2 as a target for head and neck cancer therapy. *Expert Opin Ther Targets*. 2013;17:203–216. doi:10.1517/14728222.2013.740012

32. Ali-Labib R, Louka ML, Galal IH, Tarek M. Evaluation of matrix metalloproteinase-2 in lung cancer. *Proteomics Clin Appl*. 2014;8:251–257. doi:10.1002/prca.201300086

33. Hassan M, Watari H, AbuAlmaaty A, Ohba Y, Sakuragi N. Apoptosis and molecular targeting therapy in cancer. *Biomed Res Int*. 2014;2014:150845. doi:10.1155/2014/150845

34. Elmore S. Apoptosis: a review of programmed cell death. *Toxicol Pathol*. 2007;35:495–516. doi:10.1080/01926230701320337

35. Jaiswal PK, Goel A, Mittal RD. Survivin: A molecular biomarker in cancer. *Indian J Med Res*. 2015;141:389–397. doi:10.4103/0971-5916.159250

36. Groner B, Weiss A. Targeting survivin in cancer: novel drug development approaches. *BioDrugs*. 2014;28:27–39. doi:10.1007/s40259-013-0058-x

37. Correia C, Lee SH, Meng XW, et al. Emerging understanding of Bcl-2 biology: implications for neoplastic progression and treatment. *Biochim Biophys Acta*. 2015;1853:1658–1671. doi:10.1016/j.bbamcr.2015.03.012

38. Thomas S, Quinn BA, Das SK, et al. Targeting the Bcl-2 family for cancer therapy. *Expert Opin Ther Targets*. 2013;17:61–75. doi:10.1517/14728222.2013.733001

39. Porter AG, Janicke RU. Emerging roles of caspase-3 in apoptosis. *Cell Death Differ*. 1999;6:99–104. doi:10.1038/sj.cdd.4400476

40. Galluzzi L, Kepp O, Kroemer G. Caspase-3 and prostaglandins signal for tumor regrowth in cancer therapy. *Oncogene*. 2012;31:2805–2808. doi:10.1038/onc.2011.459